ADVANCED FUNCTIONAL MATERIALS
www.afm-journal.de

Inhibition of Multidrug Resistance of Cancer Cells by Co-Delivery of DNA Nanostructures and Drugs Using Porous Silicon Nanoparticles@Giant Liposomes

Feng Kong, Xu Zhang, Hongbo Zhang, Xiangmeng Qu, Dong Chen, Mark Servos, Ermei Mäkilä, Jarno Salonen, Hélder A. Santos, Mingtan Hai, and David A. Weitz**

Biocompatible, multifunctional, stimuli responsive, and high drug loading capacity are key factors for the new generation of drug delivery platforms. However, it is extremely challenging to create such a platform that inherits all these advanced properties in a single carrier. Herein, porous silicon nanoparticles (PSi NPs) and giant liposomes are assembled on a microfluidic chip as an advanced nano-in-micro platform (PSi NPs@giant liposomes), which can co-load and co-deliver hydrophilic and hydrophobic drugs combined with synthesized DNA nanostructures, short gold nanorods, and magnetic nanoparticles. The PSi NPs@giant liposomes with photothermal and magnetic responsiveness show good biocompatibility, high loading capacity, and controllable release. The hydrophilic thermal oxidized PSi NPs encapsulate hydrophobic therapeutics within the hydrophilic core of the giant liposomes, endowing high therapeutics loading capacity with tuneable ratio and controllable release. It is demonstrated that the DAO-E A$\widehat{\mathbf{B}}$ DNA nanostructures have synergism with drugs and importantly they contribute to the significant enhancement of cell death to doxorubicin-resistant MCF-7/DOX cells, overcoming the multidrug resistance in the cancer cells. Therefore, the PSi NPs@giant liposomes nano-in-micro platform hold great potential for a cocktail delivery of drugs and DNA nanostructures for effective cancer therapy, controllable drug release with tuneable therapeutics ratio, and both photothermal and magnetic dual responsiveness.

1. Introduction

The co-delivery of molecular-targeted therapeutics for combination therapy is one of the hottest areas in biomedicine due to its ability to suppress drug toxicity and reduce drug resistance for effective cancer treatment.[1–6] Most of the targeted drugs, from monoclonal antibodies to small molecule kinase inhibitors, are still most effective in combination therapy. Combination of two or more drugs working synergistically[3,7] often produces an even greater response rate or survival time than each individual drug at its optimal dose.[8–14] In addition, the selectivity in targeting oncoproteins or oncogenes significantly enhances the treatment efficiency.[8] However, co-administration of therapeutics with high efficiency, tunable ratio, and targeting selectivity into a single carrier represents a great challenge for the encapsulation and release technological point of view. Despite remarkable progress in formulating drugs combinations, substantial obstacles such as low drug loading efficacy and low antitumor efficacy are still remained unsolved.[8]

F. Kong,[+] Dr. H. Zhang, X. Qu,[++] Prof. M. Hai
School of Materials Science and Engineering
University of Science and Technology Beijing
Beijing 100083, P. R. China
E-mail: mhai@seas.harvard.edu
Dr. X. Zhang,[+++] Dr. H. Zhang, X. Qu, Dr. D. Chen, Prof. M. Hai, Prof. D. A. Weitz
School of Applied Science and Engineering
Harvard University
Cambridge, MA 02138, USA
E-mail: weitz@seas.harvard.edu
Dr. X. Zhang, Prof. M. Servos
Department of Biology
University of Waterloo
ON N2L3G1, Canada
Dr. H. Zhang, Prof. H. A. Santos
Division of Pharmaceutical Chemistry and Technology
Faculty of Pharmacy
University of Helsinki
FI-00014 Helsinki, Finland
E. Mäkilä, Prof. J. Salonen
Laboratory of Industrial Physics
Department of Physics, University of Turku
FI-20014 Turku, Finland
[+]Present address: Grikin Advanced Materials Co. Ltd., No. 33 Chaoqian Road, Changping District, Beijing 102200, P. R. China
[++]Present address: Department of Mechanical and Electrical Engineering, Xiamen University, Xiamen 361005, P. R. China
[+++]Present address: 1250 Grand Lake Rd., Verschuren Centre, Cape Breton University, Sydney, NS, Canada

DOI: 10.1002/adfm.201500594

Liposomes and porous silicon nanoparticles (PSi NPs) are ideal delivery vehicles because of their biocompatibility and biodegradability,[15–18] and their ability to deliver both hydrophilic and hydrophobic therapeutics.[19–21] The PSi NPs can co-load both hydrophobic and hydrophilic therapeutics with high loading amounts due to their tunable pore size, large surface area, and pore volume, and simple loading procedure.[22] In addition, the encapsulation of doxorubicin hydrochloride (DOX) within the liposomes for breast cancer treatment has been shown to effectively minimize the drug's side effects.[1] However, the encapsulation of hydrophobic and hydrophilic therapeutics in giant liposomes with high efficiency and precise size control is very difficult to achieve by conventional approaches such as electroformation and hydration.[23,24] Moreover, DOX has been shown to induce multi-drug resistance in cancer cells, both in laboratory and clinical studies.[25] On the other hand, DNA nanostructures do not exhibit any obvious cytotoxicity or immunogenicity[26] and have been found to be very stable in cell lysate,[26] and have been reported to enhance the death of cancer cells[26,27] as well as shown multidrug resistance inhibition of DOX.[27,28]

Microfluidic techniques are very powerful for microencapsulation and microcapsules fabrication.[29,30] Thus, in order to create an advanced nano-in-micro platform for DNA nanostructures and therapeutics combination with high efficacy and synergism to reduce simultaneously the side effect of drugs and multidrug resistance, functional PSi NPs and core–shell multifunctional giant liposomes are assemble. Here, we synthesize hydrophilic thermally oxidized porous silicon nanoparticles (TOPSi NPs),[31] DAO-E AB̈ DNA nanostructure,[32] nano-magnetite and gold nanorods, and we co-load them with three therapeutics in monodisperse core–shell giant liposomes on a microfluidic chip. A hydrophilic therapeutic (DOX), DNA nanostructure, nano-magnetite, gold nanorods, and PSi NPs encapsulating the hydrophobic drug Erlotinib, were all encapsulated in the core of the giant liposome, whereas the hydrophobic drug 17-AAG was encapsulated in the bilayer membrane of the giant liposome. We evaluated the biocompatibility of the assembled giant liposomes in the nano-in-micro platform, demonstrated the release of the therapeutics and the other payloads from the platform, and showed the ability of the DNA nanostructure therapeutics combination on the synergistic effects and multidrug resistance inhibition.

2. Results and Discussion

2.1. Preparation of Monodisperse Multifunctional Giant Liposomes

To fabricate the giant liposomes, water-in-oil (w/o/w) emulsion templates were produced. In the giant liposomes, the hydrophilic DOX, nano-magnetite (around 15 nm by SEM; zeta-potential of +7.0 mV), gold nanorods (around 50 nm by scanning electron microscopy (SEM); zeta-potential of –0.6 mV) and the PSi NPs (particle size: 171 ± 5 nm; zeta-potential: of –35.5 ±0.9 mV)[31] were encapsulated in the core, and the hydrophobic drug 17-AAG in the bilayer membrane after solvent removal. The hydrophilic thermal oxidized PSi NPs can be loaded with both hydrophobic and hydrophilic drugs through a simple loading procedure;[31] the surface area of PSi NPs was 172 m^2 g^{-1} and the pore volume of 0.63 cm^3 g^{-1}. Thus, PSi NPs were used to promote the drug loading capacity,[6,33] enabling the co-loading of the hydrophobic drug Erlotinib within the core of the giant liposomes with tunable drug ratio. By using such approach, three or more drugs with diverse properties can be simultaneously encapsulated into the core–shell giant liposomes, as shown in **Scheme 1**. In addition, magnetite NPs and gold nanorods are also encapsulated into the platform (Scheme 1), which can endow the PSi NPs@giant liposomes with magnetic and photothermal responsiveness.[34]

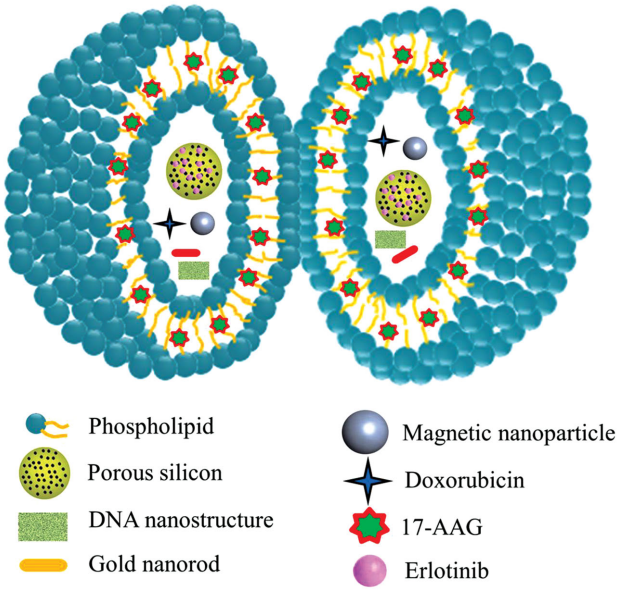

Scheme 1. Production of monodisperse core–shell giant liposomes assembled with PSi NPs as a nano-in-micro platform for co-loading and co-delivery of DNA nanostructures and drugs.

The monodisperse double-emulsion templates were fabricated according to our previous work,[24] as shown in **Figure 1**. The inner water phase contained 5–10 mg mL^{-1} of DOX solution with 10 μg mL^{-1} nano-magnetite, 1 μg mL^{-1} gold nanorods, and 500–1000 μg mL^{-1} PSi NPs loaded with Erlotinib or Erlotinib and 17-AAG. The middle oil phase contained phospholipids at the concentration of 5–10 mg mL^{-1}, together with 17-AAG concentrations up to 5 mg mL^{-1}. The outer water phase consisted of a 10 wt% PVA solution. The droplets were formed at the orifice of the collection tube where the three different phase fluids met, as shown in Figure 1a. The overall size and the thickness of the oil shell can be adjusted either by changing the flow rates of each fluid phase or by varying the capillary diameters in the device, as described previously.[23,24] The uniformity of the collected droplets is shown in Figure 1b. The giant liposomes can be formed by removing the organic solvent from the hydrophobic layer of the emulsion droplets by a dewetting process.[23,24] Figure 1c,d show the confocal image and the colorful image of the DNA nanostructures and the co-loaded drugs in the giant liposomes after solvent removal. Figure 1e,f show the fresh made giant liposomes encapsulating DOX alone and the giant liposomes after 7 d of storage.

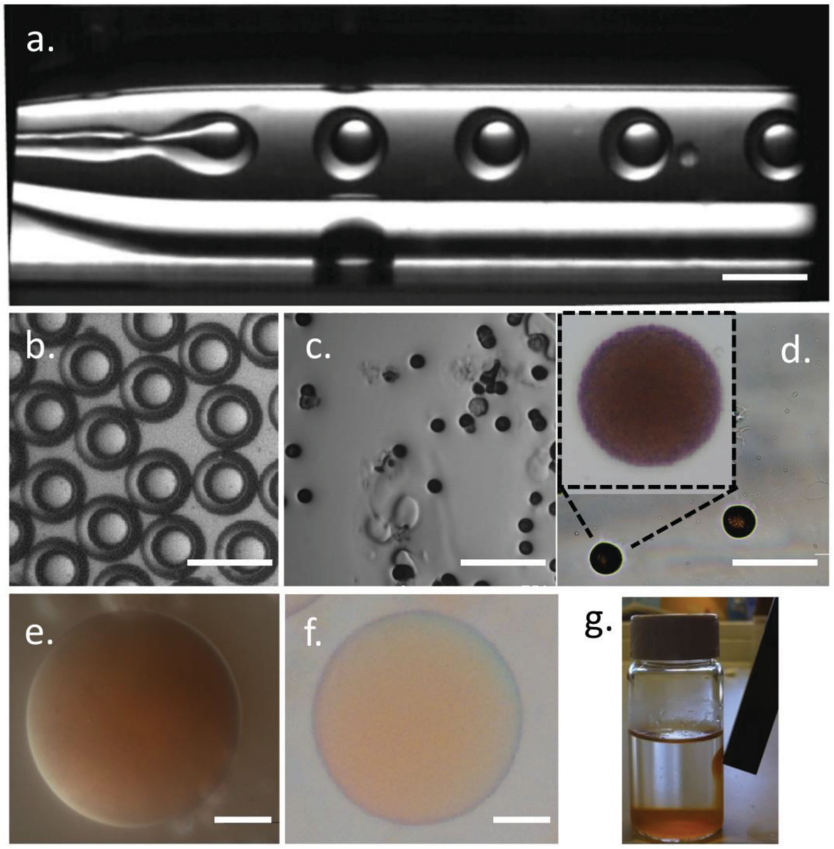

Figure 1. Preparation of w/o/w emulsion templates and formation of core–shell magnetic and photothermal-responsive PSi NPS@giant liposomes for co-loading of DNA nanostructure and drugs combination. a) Optical microscopy image of a running microfluidic device producing monodisperse double-emulsion droplets. b) Optical microscopy images of the collected w/o/w emulsion droplets co-loaded with DNA nanostructure and drugs combination. c) Colorful microscope image of the platform co-loaded with DOX+DNA+Erlotinib+17-AAG on a glass slide. d) Colorful image of the multifunctional giant liposomes formed on a glass slide. e) Colorful image of the giant liposomes encapsulating DOX alone. f) Colorful image of the release of DOX from giant liposomes 7 d after encapsulation. The scale bars in a–d) and e–f) denote 150 and 20 μm, respectively. g) Magnetic-responsive giant liposomes.

Figure 1f shows that the giant liposomes had good stability and maintained the core–shell spherical-shape even after 7 d of storage. The giant liposomes also showed good magnetic-responsive properties (Figure 1g and Video S1, Supporting Information) for potential biomedical applications.

2.2. Synthesis of Gold Nanorods and DNA Nanostructures

Short gold nanorods have unique optical properties that are exploited for photothermal therapy[35–37] and both triggered drug and protein release.[37] We synthesized 50 nm short gold nanorods coated with surfactant cethyltrimetylammonium bromide (CTAB) (**Figure 2**a) using a seed-mediated growth method. The gold nanorods of this size are responsive to wavelengths of 975 nm, which makes them particular well suited for biomedical applications since the absorbance of the surrounding tissue in this region is low.[37] Thus, the gold nanorods may endow the giant liposomes with photothermal responsive to heat and laser. Importantly, gold nanorods also exhibit high affinity to DNA nanostructure and DOX,[37] and thus, can enhance the loading of the DNA nanostructures and DOX inside the giant liposomes.[37]

The hydrophilic PSi NPs (Figure 2c) were around 170 nm in size, which can co-load hydrophobic and hydrophilic drugs, and significantly enhance the loading capacity of the hydrophobic drugs within the water core of giant liposomes with tunable drugs ratio.[6,17] In addition, PSi NPs have also been shown to have great potentials in many other biomedical applications.[38–44]

Moreover, we synthesized a 2D tile-based self-assembly DAO-E AB̈ DNA through nano- to micrometer scale.[32] The atomic force microscopy (AFM) image of the synthesized DNA nanostructures is shown in Figure 2d. Stripes of about 25 nm are clearly observed, which indicates the success in the DNA nanostructures formation (Figure 2d).[34] The DNA nanostructures have been reported to have potential to work synergistically with anticancer drugs,[27] but not tested before with DAO-E AB̈ DNA. Thus, the PSi NPs and giant liposomes assembly simultaneously encapsulated DAO-E AB̈ DNA nanostructures and different drugs, providing an excellent platform to study the synergistically effect between the DNA nanostructures and the anticancer drugs tested in this study.

2.3. DNA Nanostructures, Drug Loading, and Release

To demonstrate the high encapsulation efficiency and loading content of the drugs and the DNA nanostructures, we measured the concentration of DOX, DNA nanostructures in the inner water phase, in the collected emulsion and in the giant liposomes. The calculated encapsulation efficiency of DOX and the DNA nanostructures in the giant liposomes was 93 ± 2% and 94 ± 3%, respectively. The initial concentration of 17-AAG in the oil phase, in the collected double emulsion and in the giant liposomes was measured by liquid chromatography–mass spectrometry (LC-MS), and the calculated encapsulation efficiency of 17-AAG in the giant liposomes was 94 ± 2%. We defined the drug loading content as the weight ratio between the drug and the giant liposomes or the PSi NPs. The drug loading content of the PSi NPs for Erlotinib was about 10 wt%. We were able to tune the therapeutics ratios between DOX, Erlotinib, and 17-AAG by adjusting the drug and PSi NPs' concentration during microfluidics. The maximum drug loading content in the giant liposomes was about 30 wt% for DOX and 15 wt% for 17-AAG. The PSi NPs promoted significantly the hydrophobic drug loading capacity in the aqueous core of the giant liposomes. The encapsulation efficiency of the short gold nanorods was 95 ± 2%. The high drug loading capacity enabled the PSi NPs@giant liposomes

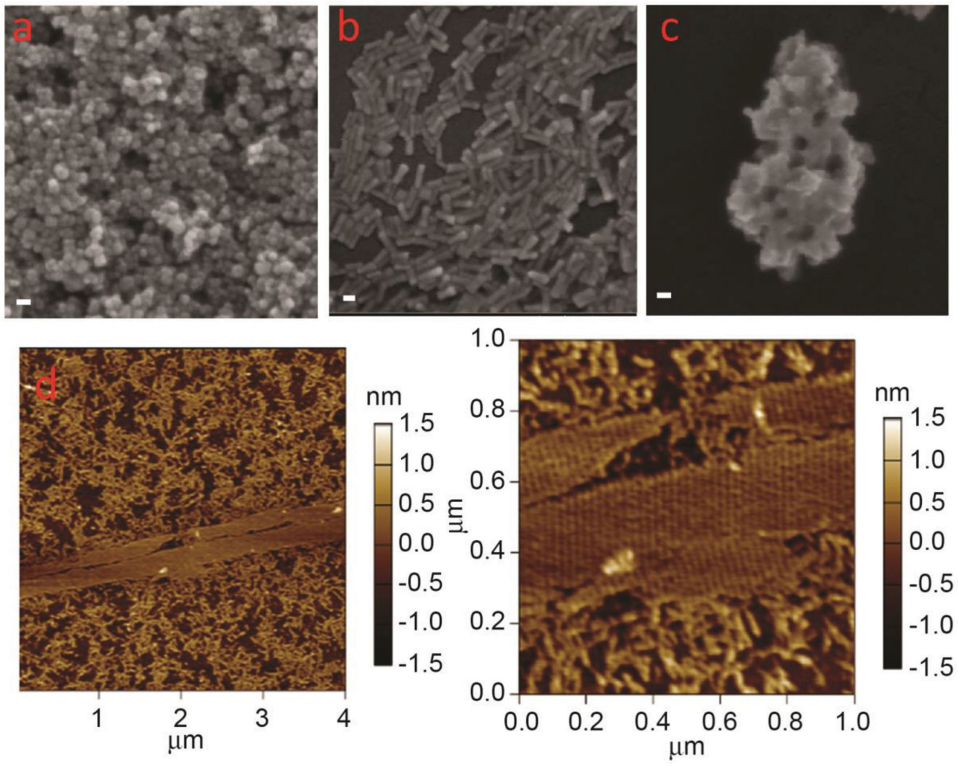

Figure 2. SEM morphology images of synthesized a) magnetic nanoparticles, b) gold nanorods, c) PSi NPs, and d) AFM image of DAO-E AB̂ DNA nanostructures with stripes about 25 nm. The scale bars denote 20 nm for (a–c).

for advanced co-delivery of DNA nanostructures and drugs with tunable drugs ratios.

The in vitro drug release profiles of free DOX solution, DOX, 17-AAG, Erlotinib, DNA nanostructures and gold nanorods loaded giant liposomes in phosphate buffer saline (PBS buffer, pH 7.4) and pH 5.2 medium are shown in **Figure 3**a,b. The drugs release from the platform in acidic environment was faster than that from neutral medium. The release studies confirmed that no initial burst release was observed for the drugs, and about 80%–90% of the drugs (DOX and 17-AAG), 80% of gold nanorods, 70%–80% of DNA nanostructures, and 50% of Erlotinib were released within 24 h in pH 7.4. The double entrapment from both the PSi NPs and the giant liposomes enabled Erlotinib to have a more sustained and controllable release.

To demonstrate the thermal function of the gold nanorods, the release of DOX from the platform with and without gold nanorods was performed at 37 °C, 45 °C, and 55 °C (Figure 3c,d). The heat release confirmed that the DOX release from the platform containing gold nanorods slightly increased with the temperature due to the heat responsiveness of the gold nanorods. The photothermal response of the gold nanorods can be subjected to laser irradiation at the site of the tumor, and thus, achieve targeted drug release. In addition, gold nanorods are also themselves therapeutics for cancer, which have shown potential in extracellular hyperthermia cancer therapy[37] (using local heating at above 42≈43 °C for tumor ablation) both in vitro and in vivo, as well as it has also been shown that gold nanorods can inhibit cancer cell migration.[45]

The giant liposomes had a shell thickness of a few nanometers and acted as a membrane system for the small drugs and the DNA nanostructures to diffuse through it. The release of DOX from the giant liposomes was much slower than the DOX solution, as expected. Moreover, 17-AAG and Erlotinib are insoluble in the release buffer, thus by encapsulating 17-AAG in the phospholipid bilayer and Erlotinib inside the PSi NPs in the core of the giant liposomes, the solubility of the drugs was significantly enhanced, and a simultaneous controllable release of Erlotinib from the PSi NPs was also achieved. The sustained drug release was not affected by the encapsulation of the magnetic nanoparticles, short gold nanorods, DNA nanostructures, and PSi NPs inside the giant liposomes (data not shown).

2.4. Cytotoxicity Studies

To confirm the cytocompatibility of the PSi NPs@giant liposomes platform, the in vitro cell viability studies were conducted in human cervical HeLa cells, and human breast cancer MCF-7 cells, DOX-resistant human breast cancer MCF-7/DOX cells, and M28 cells, using a two-colored live/dead assay. The green color stained by Calcein AM indicates that the cells are live and the red color stained by EthD-1 indicates that the cells are dead. The cell viability in response to the platform at different concentrations on HeLa, M28, MCF-7, and MCF-7/DOX cells after 24 h of incubation at 37 °C is shown in **Figure 4**a. The platform containing 10 µg of magnetite, 1×10^{-9} M of gold nanorods and 500 µg mL^{-1} of PSi NPs showed good

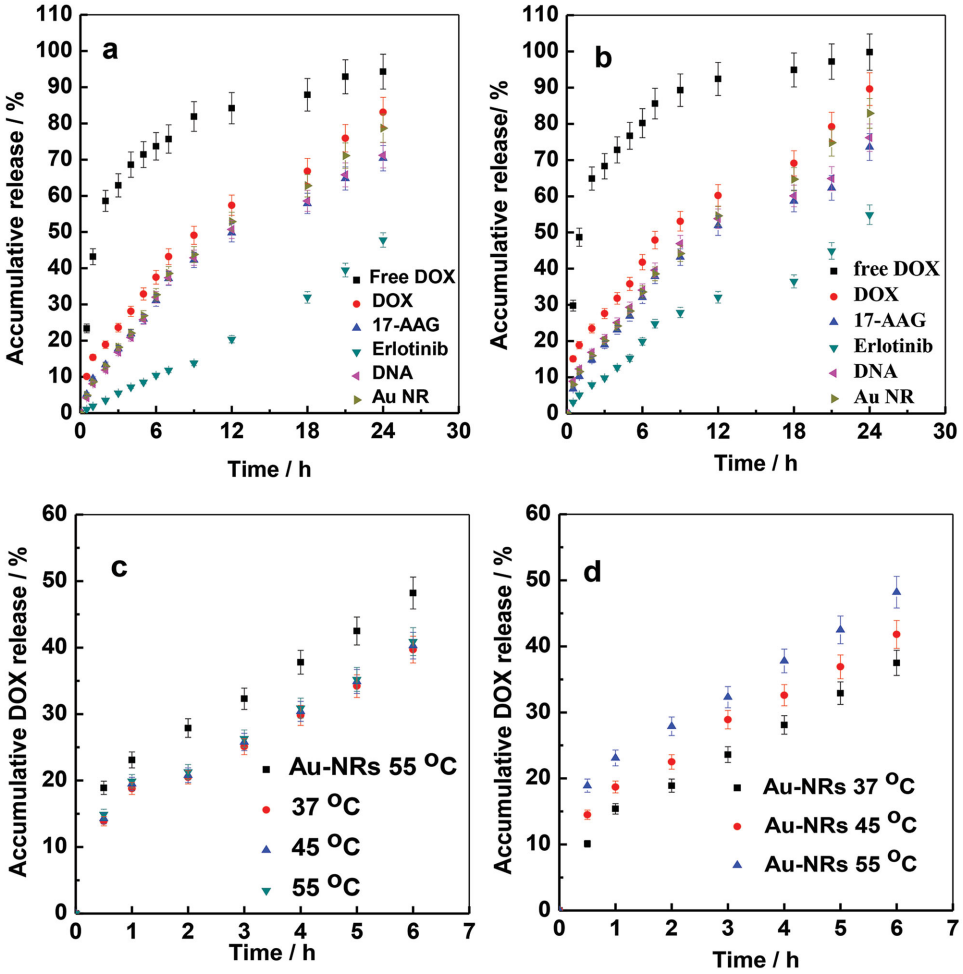

Figure 3. In vitro release of the different compounds loaded in the PSi NPs@giant liposome platform. a) The in vitro release studies conducted at pH 7.4 in medium at 37 °C. b) The in vitro release studies conducted at pH 5.2 in medium at 37 °C. c) The thermal release of DOX from the PSi NPs@giant liposome platform without gold nanorods at 37 °C, 45 °C, and 55 °C, and with gold nanorods (1×10^{-9} M) at 55 °C. d) The thermal release of DOX from the PSi NPs@giant liposome platform with gold nanorods (1×10^{-9} M) at 37 °C, 45 °C, and 55 °C.

cytocompatibility to all the studied cell lines after 24 h of incubation at 37 °C (Figure 4a). Figure 4b shows the MCF-7 cell viability in the presence of the giant liposomes after 48 h incubation at 37 °C. Figure 4c shows the cytotoxicity of the prepared giant liposomes in HeLa NucLight Red cell using a two-color Cytotoxicity Demo kit at 37 °C after 24 h of incubation. All cell viability and cytotoxicity results confirmed that the prepared giant liposomes and PSi NPs assembled nano-in-micro platform were cytocompatible in the different cancer cell lines.

2.5. Enhanced Drug Efficacy Studies

To confirm that the encapsulation of DOX in the nano-in-micro platform with and without magnetic and photothermal responsiveness could reduce the effect of DOX, the amount of dead M28 cells, which represent a non-carcinoma human cell, were treated with free DOX solution, and both DOX-loaded and DOX+17-AAG-loaded PSi NPs@giant liposomes with and without 10 μg mL^{-1} of nano-magnetite and 1 μg mL^{-1} of gold nanorod suspensions after 24 h incubation at 37 °C. The results measured with either AlamarBlue or live/dead assays are shown in **Figure 5**a. The M28 dead cells treated by either DOX or the DOX+17-AAG-loaded PSi NPs@giant liposome platform were much lower than those of free DOX at the same DOX concentration, indicating that the effect of DOX was reduced when encapsulated in the PSi NPs@giant liposome platform with and without magnetic-photothermal responsiveness.

DOX is one of the most effective anticancer drug for the treatment of breast cancer, but the bioavailability of DOX through oral administration route is rather low (<5% in mice) due to its systemic toxicity, making the development of an oral DOX delivery system that uses it synergistically with other therapeutics of particular importance. Oral delivery of DOX using novel liposomes has revealed a 5.94-fold increase in oral bioavailability of DOX,[1] exhibiting a remarkable reduction of the drug's side effects;[46] however, the encapsulation efficiency was only about 60%.[1] On the other hand, 17-AAG and Erlotinib are drugs, which actively target HER2 and EGFR oncogenes, thus the combination of DOX, Erlotinib,

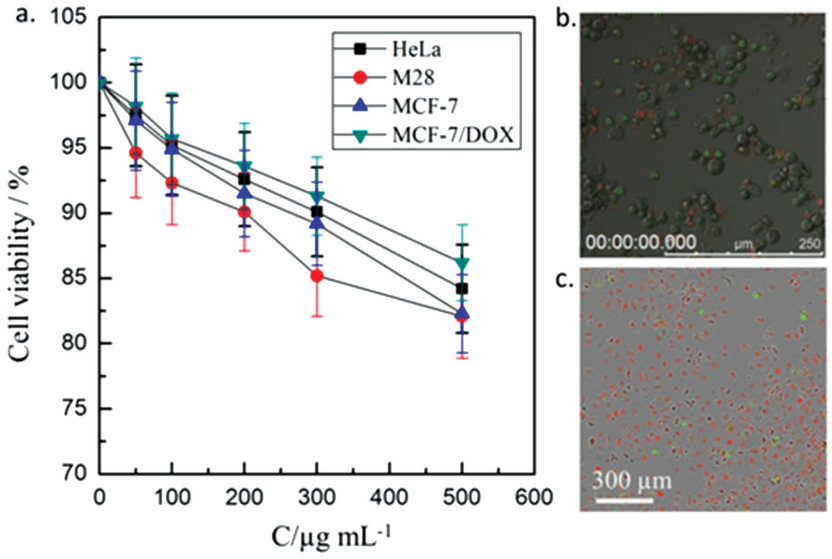

Figure 4. In vitro cell viability/cytotoxicity studies of the multifunctional giant liposomes. a) Cell viability of HeLa, M28, MCF-7, and MCF-7/DOX cells exposed to the PSi NPs and the multifunctional giant liposomes platform (containing 10 μg mL^{-1} of nano-magnetite and 1×10^{-9} M of gold nanorods and 500 μg mL^{-1} PSi NPs) at different concentrations for 24 h incubation at 37 °C using a live/dead assay. b) Confocal image of 100 μg mL^{-1} giant liposomes suspension on HeLa cells after 48 h incubation at 37 °C using a live/dead kit Calcein AM and EthD-1. c) Cell cytotoxicity test of the prepared giant liposomes suspensions on HeLa NucLight Red cells after 24 h incubation at 37 °C using two-colored Cytotoxicity Demo kit.

and 17-AAG is hypothesized to affect the treatment of HER2 or EGFR-driven breast cancer. Moreover, the nano-in-micro platform for co-delivery of synergistic drug combinations with targeting selectivity would enhance the drug effectiveness, suppress the drug resistance, and possibly reduce the side effects of the drugs by improving their pharmacokinetics. Figure 5b shows that the combined drugs had higher cytotoxicity than any single drug at all dose levels tested in the MCF-7 cells, indicating that the drugs combination can indeed enhance the drug's anticancer efficiency. Moreover, DNA nanostructures and drugs combination showed a significantly better anticancer efficiency than the single drugs. The combination of DOX+17-AAG, DOX+Erlotinib, and DOX+17-AAG+Erlotinib can thus induce effectively MCF-7 cell death through such drug synergism effect.

2.6. Synergism of DNA Nanostructures and Drugs Combination

Two or more drugs combined in one single carrier provide a two-in-one punch to knock the cancer cells out and is usually more efficient than a single drug molecule.[47] In addition, the combination of drugs and other therapeutics might induce better cancer treatment efficiency. To demonstrate the synergistic effect of the drugs and the DNA nanostructures co-loaded PSi NPs@giant liposomes, the in vitro cell viability/cytotoxicity studies of the single drugs alone and drug combinations

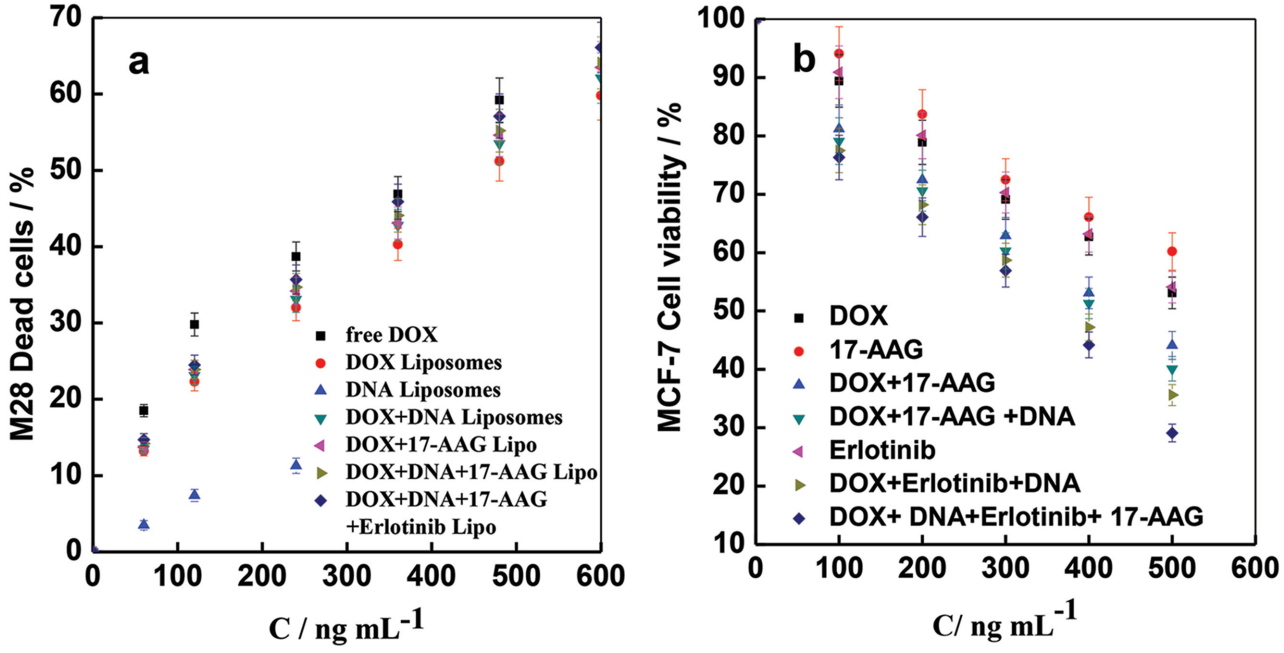

Figure 5. Drug side effect reduction of the nano-in-micro platform. a) Drug–cell proliferation study. The M28 dead cells (noncarcinoma cells) by DOX in water solution, DOX in giant liposome, DNA nanostructure, DOX+DNA, DOX+17-AAG+DNA+erlotinib loaded giant liposome platform after 24 h incubation at 37 °C using an AlamarBlue assay. b) Cell proliferation profiles in the presence of free drugs, DNA nanostructure combination loaded nano-in-micro platform on MCF-7 cells after 24 h incubation at 37 °C using an AlamarBlue assay.

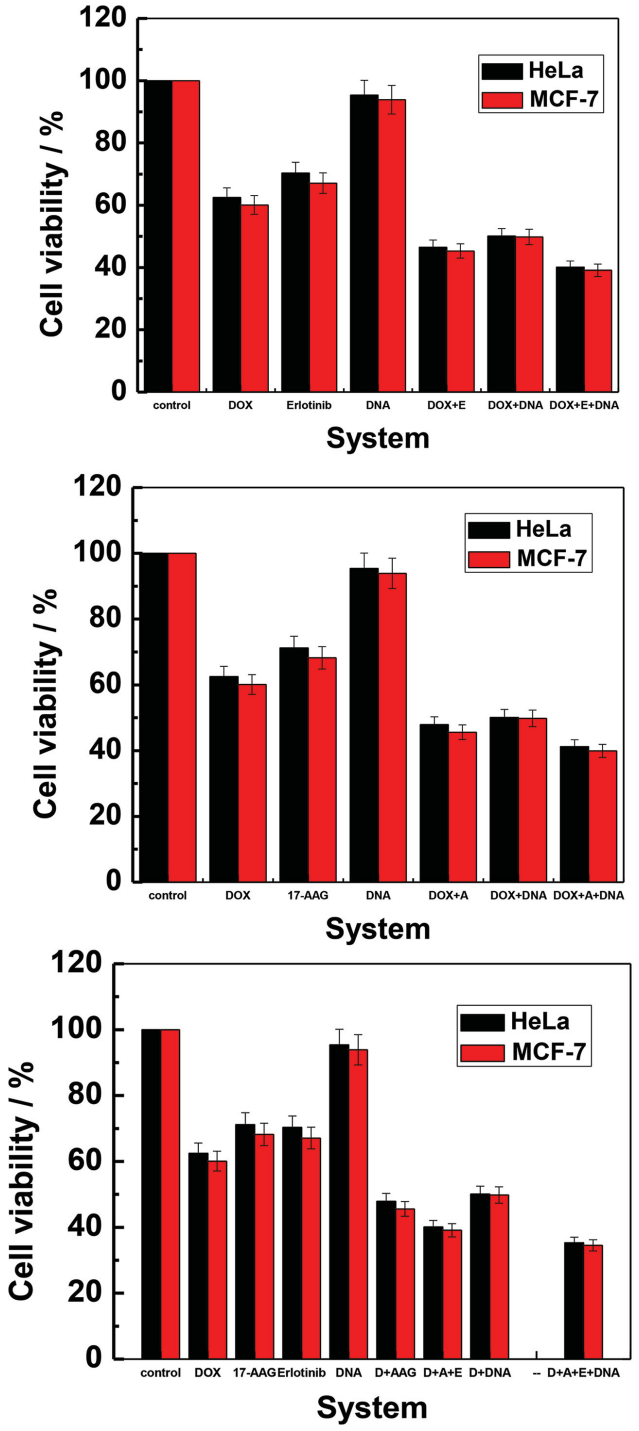

Figure 6. The synergistic effect of DNA and drugs on the cancer cells viability. The synergistic effect of drugs combination and DNA nanostructure combination on HeLa and MCF-7 cell lines after 24 h incubation ($C_{DOX}/C_{17\text{-}AAG}/C_{Erlotinib}$ = 2:1:1; $C_{DOX}/C_{17\text{-}AAG}$ = 2:1; $C_{DOX}/C_{Erlotinib}$ = 2:1; the total concentration of the drug/drugs was 360 ng mL^{-1}; giant liposomes co-loaded with 10 μg mL^{-1} nano-magnetite, 1 × 10^{-9} M gold nanorods and 500 μg mL^{-1} PSi NPs) using a live/dead assay. (Untreated cells in giant liposomes with 10 μg mL^{-1} nano-magnetite, 1 × 10^{-9} M gold nanorods and 500 μg mL^{-1} PSi NPs were used as controls). Data were presented as the average of three measurements with ± standard deviation (n = 3).

DOX+17-AAG, DOX+DNA, DOX+17-AAG+Erlotinib, and DOX+DNA+17-AAG+Erlotinib on both HeLa and MCF-7 cells, were conducted. The free DOX solution was used as control. **Figure 6** shows the HeLa and MCF-7 cell viabilities after 24 h of incubation at 37 °C with single drug-, multidrug-loaded and DNA nanostructures combination loaded in the platform. At the same drug concentration, drug combinations and DNA nanostructures combination induced more cell death than each single drug used alone, showing the synergistic effect between the different compounds. DNA nanostructures enhanced the efficiency of single DOX, as well as the drug combination. The calculated combination index (CI), indicating the type and amount of interaction between two or more drugs with respect to the experimental parameters (IC_{50}),[48] is shown in **Figure 7**, which represents that the combination of DOX and 17-AAG or DOX and Erlotinib had a synergistic effect on cell death. The synergism between DOX and 17-AAG on breast cancer MCF-7 cells death was slightly stronger than that of DOX and Erlotinib.

2.7. Inhibition of Multidrug Resistance

To investigate the enhanced inhibition against multidrug resistant in cells caused by DNA nanostructures and drugs combination, the DOX-resistant MCF-7/DOX cells (a model multidrug resistance inhibition cell) were incubated for 24 h at 37 °C in the presence of DOX, 17-AAG, DNA nanostructures, DOX+17-AAG, DOX + DNA, DOX + Erlotinib, DOX+17-AAG+DNA, and DOX + Erlotinib+17-AAG +DNA loaded platforms containing 10 μg mL^{-1} of nanomagnetite, 1 × 10^{-9} M of gold nanorods, and 500 μg mL^{-1} of PSi NPs. As shown in **Figure 8**, DOX alone exhibited a rather low cytotoxicity, which indicated a high drug resistance of the cells to DOX. DNA nanostructures and drugs combination exhibited enhanced cytotoxicity on MCF-7/DOX cells. Moreover, the

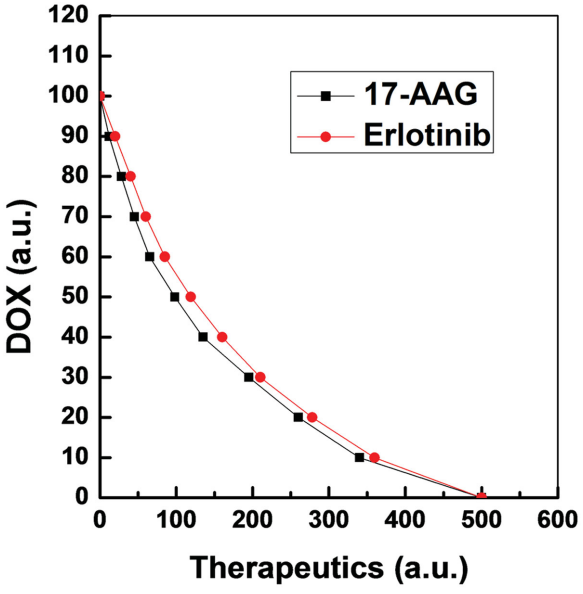

Figure 7. Isobologram. Abscissa and ordinate units are the concentrations of the drugs DOX, 17-AAG, and Erlotinib.

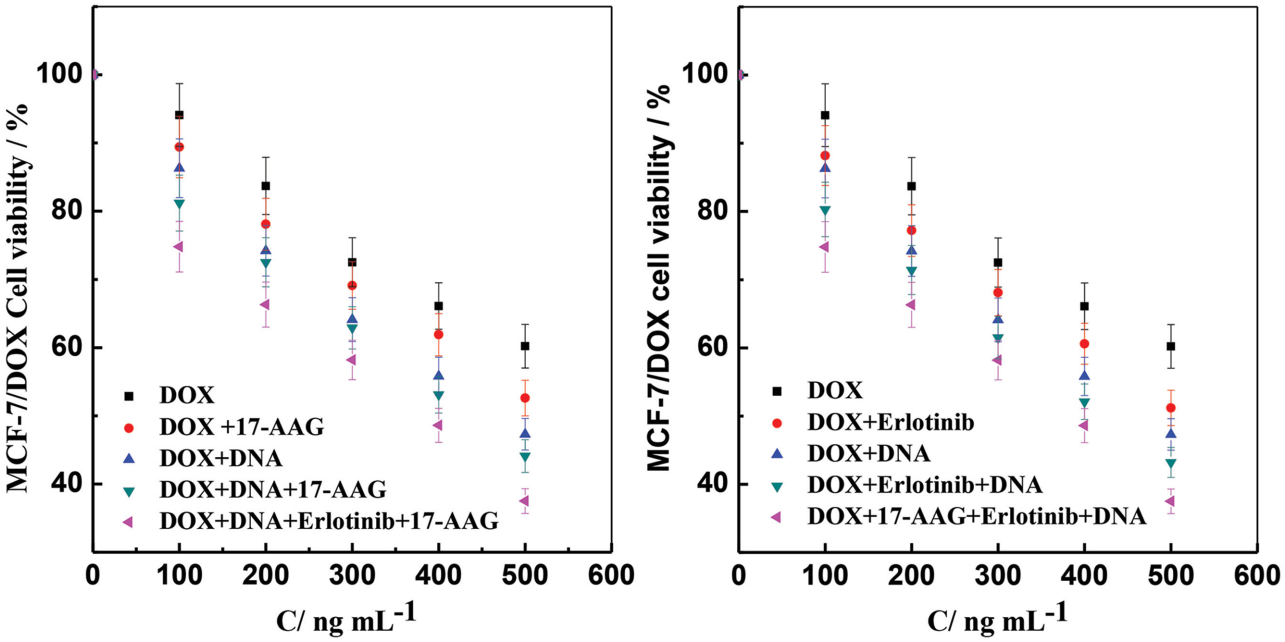

Figure 8. In vitro multidrug resistance inhibition study. The cell viability of DOX, 17-AAG, Erlotinib, DNA nanostructure, DOX+17-AAG, DOX+DNA, DOX+DNA+Erlotinib, DOX+DNA+Erlotinib+17-AAG-loaded platform ($C_{DOX}/C_{17\text{-}AAG}/C_{Erlotinib}$ = 2:1:1; $C_{DOX}/C_{17\text{-}AAG}$ = 2:1; $C_{DOX}/C_{Erlotinib}$ = 2:1;giant liposomes loaded with 10 μg mL^{-1} nano-magnetite, 1 × × 10^{-9}M gold nanorods and 500 μg mL^{-1} PSi NPs) was determined on DOX-resistant MCF-7/DOX cells for 24 h incubation at 37 °C using a live/dead assay (untreated cells in giant liposomes containing 10 μg mL^{-1} of nano-magnetite, 1 × 10^{-9} M of gold nanorods and 500 μg mL^{-1} of PSi NPs were used as controls).

drugs and DNA combination induce more MCF-7/DOX cell death than that of drugs combination at the same drug concentration and same ratio. These results confirmed that the developed biocompatible nano-in-micro platform can effectively lead to death of even multidrug resistance cells and enhance the drugs' effect compared to single drugs alone. Most importantly, the DNA nanostructures loaded in the platform contributed to the significant enhancement of MCF-7/DOX cell death when combined with different drugs. As reported in the literature, the short DNA oligonucleotides with no special sequence do not have therapeutic effect. The DNA has to form nanostructures in order to produce effects on multidrug resistance inhibition.[27,28]

3. Conclusion

We synthesized PSi NPs, magnetic NPs, gold nanorods, and DNA nanostructures, and created monodisperse biodegradable PSi NPs@giant liposomes as an advanced co-delivery nano-in-micro biocompatible platform for the combination of DNA nanostructures and drugs on a microfluidic chip. The platform shows magnetic and thermal responsive. PSi NPs carry the hydrophobic therapeutics within the core of the giant liposomes and promote the system with high drug loading capacity, as well as sustain the release of the therapeutics with tunable therapeutics ratio. The nano-in-micro platform is of excellent cytocompatibility, enabled the co-delivery of DOX, 17-AAG, Erlotinib drugs, as well as DNA nanostructures, thus achieving a synergistic effect. Importantly, the DNA nanostructure and therapeutics combination contributed to the significant enhancement on the DOX-resistant MCF-7/DOX cell death, thus inhibiting the multidrug resistance. Overall, the PSi NPs@giant liposome platform holds great potential for a cocktail delivery of drugs and DNA nanostructures for effective cancer therapy, controllable drug release with tunable therapeutics ratio, and simultaneously photothermal and magnetic dual-responsiveness.

4. Experimental Section

Materials: The inner phase of w/o/w double-emulsion droplets was made of either DOX+PVA water solution or DOX+nanomagnetite + gold nanorods + DNA nanostructures + PVA solution (PVA with molecular weight 13 000 to 23 000, 87%–89% hydrolyzed, Sigma–Aldrich). Doxorubicin hydrochloride (DOX), 17-AAG, and Afatinib were purchased from LC Laboratories. Experiments were conducted with the following lipids: 1-palmitoyl-2-oleoyl-sn-glycero-3-phosphocholine (POPC), 1,2-dioleoyl-sn-glycero-3-phosphocholine (DOPC). All phospholipids were purchased from Avanti Polar Lipids. DOPC or POPC was in liquid form with 10 mg DOPC or POPC/mL choloroform. 1,2-Dipalmitoyl-sn-glycero-3-phosphocholine (DPPC), 1,2-distearoyl-sn-glycero-3-phosphocholine (DSPC), POPC, and DOPC were purchased from Avanti Polar Lipids in powder form. $FeCl_2$, $FeCl_3$, and $NH_3{\cdot}H_2O$ were purchased from Sigma–Aldrich and used without further purification. The outer phase was either a 10 wt% PVA solution with 100 mOsm L^{-1} osmolarity. Toluene and chloroform were purchased from Sigma–Aldrich. HeLa, MCF-7, and M28 cell lines were purchased from American-Type Culture Collection. Dulbecco's modified eagle's medium (DMEM), F12, heat-inactivated fetal bovine serum (FBS), 1% penicillin-streptomycin, AlamarBlue, and live/dead kit were purchased from Invitrogen Life Technologies. 96-well black clear bottom cell culture plates were purchased from Corning Inc. Solutions and solvents were filtered by 0.2 μm membrane (Anodisc or Whatman plc.) before introduction into

glass capillary devices. Highly purified distilled water was acquired from a Millipore Milli-Q system.

Synthesis of Short Gold Nanorods: Gold nanorods were synthesized by seed-mediated growth. Gold seeds and short gold nanorods were prepared according to the same procedure, as described elsewhere.[37] Gold NR was determined by transmission electron microscopy (TEM). The gold NR-CTAB were washed twice by centrifuging at 14 100 rpm for 10 min to remove excess reactants, resuspended in Milli-Q-purified water, and kept at room temperature before further experiments. The Au NR-CTAB concentration was determined from the UV–vis spectrum (Cary 100 UV–vis spectrophotometer, Agilent Technologies) and known extinction coefficients. Au NR concentration in the experiments was about 1×10^{-9} M. The ratio between DOX and gold nanorod concentration is kept from 2000:1 to 10000:1.

Synthesis of DAO-E AB̂ DNA and AFM Imaging: DNA sequences of DAO-E AB̂ DNA nanostructure[32] have been designed by Seeman. All oligonucleotides were purchased from IDT, Inc. and purified by 20% denaturing PAGE. The strands of oligonucleotides were mixed stoichiometrically and dissolved to 0.5×10^{-6} M in 1 × TAE/Mg^{2+} buffer (40×10^{-3} M Tris-HCl (pH 8.0), 1×10^{-3} M EDTA, 3×10^{-3} M Na^{+}, 12.5×10^{-3} M Mg^{2+}), 50 µL of 0.5×10^{-6} M DNA in 1 × TAE/Mg^{2+} buffer was slowly cooled from 95 °C to room temperature over 48 h. 10 µL was spotted onto freshly cleaved mica, and left for 2 min, the sample drop was then washed off by 50 µL deionized water and dried by compressed air. DNA samples and was imaged by tapping-mode AFM on Asylum-2 MFP-3D Coax AFM with NSC15 tips (silicon cantilever, MikroMasch).

Generation of w/o/w Double Emulsions: We used glass capillary microfluidic devices to produce giant liposomes with a shell composed of phospholipids and hydrophobic 17-AAG, and a core containing the water-soluble anticancer drug DOX alone or with nanomagnetite, gold nanorods, DNA nanostructure, PSi NPs encapsulating Erlotinib. The round capillaries with inner and outer diameters of 0.58 µm and 1.0 mm were purchased from World precision instruments, Inc., and tapered to desired diameters with a micropipette puller (P-97, Sutter Instrument, Inc.) and a microforge (Narishige international USA, Inc.).[24] The tapered round capillaries were fitted into square capillaries (Atlantic International Technology, Inc.) with an inner dimension of 1.0 mm for alignment.[23] The outer diameter of the double emulsion varied from 30 to 50 µm, while the inner diameter varied from 20 to 30 µm. These values were controlled by the size of the capillaries used and the flow rates of different phases. The typical flow rates for generating w/o/w emulsion for the inner, middle, and outer phase were 500, 1100, and 2500 µL h^{-1}, respectively, and the double-emulsion droplets generation frequency was about 500 Hz. The total phospholipids concentration in the middle oil phase was controlled from 6–10 mg mL^{-1}. The concentration of DOX in the inner water phase was up to 10 mg mL^{-1}, Erlotinib in PSi NPs up to 1 mg mL^{-1}, and 17-AAG in the middle phase was up to 6 mg mL^{-1}. The nanomagnetite concentration is about 10–100 µg mL^{-1}. The concentration of DNA nanostructure and gold nanorods is about 10×10^{-9} M and 1×10^{-9} M.

Characterization of the Giant Liposomes: Colorful, bright-field and fluorescence images were obtained with 60×, 40×, 15×, and 10× objectives at room temperature using Nikon Eclipse TE-2000E or inverted fluorescence confocal microscope (Lecia, DMIR or DMIRBE) with a high-speed cameras (Phantom v7.3, v7, and v5) or digital camera (QImaging, QICAM 12-bit). All double-emulsion generation processes were monitored with the microscope either with a high-speed camera or a digital camera. The giant liposomes encapsulating either single anticancer drug or multiple drugs with and without nano-magnetite were imaged by either Nikon TE2000-E microscopy or confocal microscope.

Drug Encapsulation Efficiency Determined by UV–Vis and Liquid LC-MS: The initial concentration of DOX in the inner water phase and in the collected w/o/w emulsion was measured by UV–Vis spectrophotometer (NanoDrop ND-1000) at 234 nm. The drug encapsulation efficiency was calculated based on the percentage of the real encapsulated drug and the initial drug concentration. The concentration of 17-AAG, Erlotinib, and Afatinib was analyzed by injecting 20 µL of each diluted sample into Agilent 1200 HPLC/MDS Sciex 3200 Q-trap tandem MS system in negative electro-spray mode for quantification using water and acetonitrile as a mobile phase. The drug loading content was calculated based on the weight ratio between the drug and hybrid polymersomes. The fluorescence intensity of DNA nanostructures was measured by microplate reader (SpectraMax i3, Molecular device). The concentration of DNA in the hybrid polymersomes and in the release buffer solution was calculated based on the fluorescence intensity according to the standard DNA curves by microplate reader.

In Vitro Dynamic Drug Release: In vitro release of free DOX water solution, DOX, DNA nanostructure, Erlotinib, Au-NR, 17-AAG-loaded giant liposomes with and with nano- magnetite and gold nanorods were evaluated by a dynamic dialysis method. Aliquot of each drug-loaded or DNA+drugs-loaded suspensions PBS solution 0.8–1 mL was placed in the mini dialysis kits (2 mL, MWCO 8 kDa cut-off) (GE Health, USA) and floated in 100 mL PBS release medium or pH 5.2 buffer release medium and maintained at 37 °C with a paddle revolution speed of 100 r min^{-1} using G24 Environmental incubator shaker (New Brunswick Scientific Co. Inc.). At intervals, 500 µL of release sample was withdrawn and 500 µL fresh release medium was added to the bulk solution. The concentration of Erlotinib from the release sample was analyzed by HPLC (Agilent 1200). The concentration of DOX was measured and calculated from the maximum peak by UV–VIS spectrum at 234 nm (ND-1000 nanodrop). The concentration of DNA nanostructures was detected by microplate reader.

Cytotoxicity of the Giant Liposomes: HeLa (a human cervical carcinoma cell line), MCF-7 (human breast carcinoma line), MCF-7/DOX (doxorubicin-resistant breast cancer cell line), and M28 (human mesothelioma cell line) were maintained in DMEM supplemented with 10% heat-inactivated FBS and 1% penicillin-streptomycin (PS). The cell medium was filtered through a 0.2 µm filter. We used AlamarBlue assay or live/dead assay to determine the cell viability of giant liposomes with and without water-soluble nano-magnetite and gold nanorods (10 µg mL^{-1} nano-magnetite and 1×10^{-9} M gold nanorods) as well as 500 µg mL^{-1} PSi NPs encapsulating drugs with different concentration on HeLa cell, MCF-7, MCF-7/DOX, or M28 cell lines by using 96-well black clear bottom culture plates (Costar, Corning). HeLa, MCF-7, MCF-7/DOX, and M28 cell lines were maintained in cell culture medium. 100 µL cell medium (F12+10% FBS+1% PS) containing HeLa cells, MCF-7, MCF-7/DOX, or M28 cells with or without multifunctional giant liposomes at concentration with and without 10% (v/v) AlamarBlue were seeded on 96-well black culture dishes at a density of 1×10^4 cell mL^{-1} in an atmosphere of 5% CO_2 at 37 °C and cultured for 24 h. YOYO-1 detects the cytotoxicity by binding to the dsDNA following loss of cell membrane integrity and changing of the color of the HeLa NucLight red cells from red (live) to green (dead). The fluorescence intensity was measured at the excitation wavelength of 544 nm and emission wavelength of 590 nm by endpoint method using a microplate reader SpectraMax M2 or i3 (Molecular device). The fluorescence intensity of blank, negative control and samples are measured at 590 nm at 37 °C.

Live and Dead Assay: 100 µL of 1×10^{-6} M Calcein AM + 2×10^{-6} M of EthD-1 culture medium were added to 100 µL cell medium containing either HeLa, MCF-7 cells, MCF-7/DOX, or M28 cells with or without multifunctional giant liposomes suspensions seeded on 96-well culture plates at a density of 1×10^4 cell mL^{-1} in an atmosphere of 5% CO_2 at 37 °C and cultured for 24 h. The cell number and density were counted by Invitrogen Countess automated cell counter. The fluorescence intensity was measured at the excitation wavelength of 488 nm excitation for Calcein AM and 544 nm for EthD-1, and the emission wavelength was 530 nm for Calcein AM and 610 nm for EthD-1 using a microplate reader SpectraMax M2 or i3 (Molecular device). The cell viability of multifunctional giant liposomes on HeLa, MCF-7, MCF-7/DOX, or M28 cells was calculated based on the negative control, blank control, and samples fluorescence intensity according to live/dead assay using the following equation:

$$\% \text{ Live cells} = \frac{\left[F(530\text{ nm})_{\text{sample}} - F(530\text{ nm})\text{min}\right]}{\left[F(530\text{ nm})_{\text{max}} - F(530\text{ nm})_{\text{min}}\right]} \times 100\% \quad (1)$$

A two-colored apoptosis/cytotoxicity Demo kit from Essen BioScience and Essen's CellPlayer HeLa NucLight Red cell lines were used to study the cytotoxicity of the giant liposomes with different concentration according to the protocols. We seeded a 96-well plate with 2500 cells per well and immediately placed the 96-well plate in IncuCyte ZOOM (ESSEN BIOSCIENCE) and set the scan schedule every hour using multiple channel phase, red and green incubated at 37 °C. HeLa NucLight red cell was maintained in F12-K culture medium containing 10% FBS and 1% PS.

Multidrug Resistance Test: 96-well culture plates (Costar, Corning Corp.) were used to study the multidrug resistance of single, multiple therapeutics and DNA nanostructure drugs combination encapsulated in the multifunctional giant liposomes on doxorubicin-resistant MCF-7/DOX cells using the live/dead assay. The same protocol was used as described above.

Statistical Analysis: All the experiments in this study were performed independently at least three times and the data were expressed as the mean average ± standard deviation (s.d.).

Supporting Information

Supporting Information is available from the Wiley Online Library or from the author.

Acknowledgements

F.K., X.Z., H.Z., and X.Q. contributed equally. The authors are grateful to the Fundamental Research Funds for the Central Universities (No. FRF-BR-09–021B), 863 program of PR China (No. 2006AA03Z108); NSF (DMR-1310266) and Harvard MRSEC (DMR-0820484) for financial support. Dr. X.Z. appreciates the support from Canadian Institutes of Health Research. Dr. H.Z. acknowledges Finnish Cultural Foundation and Jane and Aatos Erkko Foundation (grant no. 4704010) for financial support. X.Q. acknowledges financial support from China Scholarship Council. Prof. H.A.S. acknowledges financial support from the Academy of Finland (grants no. 252215, 256394, and 281300), the University of Helsinki Research Funds, Biocentrum Helsinki, and the European Research Council (grant no. 310892). The authors thank Harvard CNS and FAS centers for providing the facilities for the cell experiments, AFM, SEM, and TEM imaging. The authors thank Essen BioScience for providing HeLa NucLight Red cells and two color apoptosis/cytotoxicity Demo kit and IncuCyte ZOOM for the in vitro cell apoptosis/cytotoxicity measurements. The authors acknowledge Dr. Sunia A.Trauger from Small Molecular Mass Spectrometry Facility in Harvard University for providing HPLC instrument.

Received: February 11, 2015
Revised: March 24, 2015
Published online: April 27, 2015

[1] S. Jain, S. R. Patil, N. K. Swarnakar, A. K. Agrawal, *Mol. Pharm.* **2012**, *9*, 2626.
[2] A. K. Iyer, G. Khaled, J. Fang, H. Maeda, *Drug Discovery Today* **2006**, *11*, 812.
[3] M. Shi, K. Ho, A. Keating, M. S. Shoichet, *Adv. Funct. Mater.* **2009**, *19*, 1689.
[4] V. P. Torchilin, *Nat. Rev. Drug Discovery* **2005**, *4*, 145.
[5] D. Liu, H. Zhang, B. Herranz-Blanco, E. Mäkilä, V. P. Lehto, J. Salonen, J. Hirvonen, H. A. Santos, *Small* **2014**, *10*, 2029.
[6] H. Zhang, D. Liu, M. A. Shahbazi, E. Mäkilä, B. Herranz-Blanco, J. Salonen, J. Hirvonen, H. A. Santos, *Adv. Mater.* **2014**, *26*, 4497.
[7] T. M. Allen, P. R. Cullis, *Science* **2004**, *303*, 1818.
[8] B. Al-Lazikani, U. Banerji, P. Workman, *Nat. Biotechnol.* **2012**, *30*, 679.
[9] K. C. R. Bahadur, P. Xu, *Adv. Mater.* **2012**, *24*, 6479.
[10] S. M. Lee, H. Park, K. H. Yoo, *Adv. Mater.* **2010**, *22*, 4049.
[11] T. C. Chou, *Cancer Res.* **2010**, *70*, 440.
[12] F. Greco, M. J. Vicent, *Adv Drug Delivery Rev.* **2009**, *61*, 1203.
[13] L. Mao, H. Wang, M. Tan, L. Ou, D. Kong, Z. Yang, *Chem. Commun.* **2012**, *48*, 395.
[14] Y. Chen, Y. Gao, H. Chen, D. Zeng, Y. Li, Y. Zheng, F. Li, X. Ji, X. Wang, F. Chen, Q. He, L. Zhang, J. Shi, *Adv. Funct. Mater.* **2012**, *22*, 1586.
[15] J. Wu, A. Lee, Y. Lu, R. J. Lee, *Int. J. Pharm.* **2007**, *337*, 329.
[16] Y. Niikura, S. Ohta, K. J. Vandenbeldt, R. Abdulle, B. F. McEwen, K. Kitagawa, *Oncogene* **2006**, *25*, 4133.
[17] D. Liu, H. Zhang, E. Mäkilä, J. Fan, B. Herranz-Blanco, C. F. Wang, R. Rosa, A. J. Ribeiro, J. Salonen, J. Hirvonen, H. A. Santos, *Biomaterials* **2015**, *39*, 249.
[18] B. Herranz-Blanco, D. Liu, E. Mäkilä, M.-A. Shahbazi, E. Ginestar, H. Zhang, V. Aseyev, V. Balasubramanian, J. Salonen, J. Hirvonen, H. A. Santos, *Adv. Funct. Mater.* **2015**, *25*, 1448.
[19] L. Xiao, P. Rasouli, D. M. Ruden, *Curr. Med. Chem.* **2007**, *14*, 223.
[20] V. P. Torchilin, *Adv. Drug Delivery Rev.* **2006**, *58*, 1532.
[21] Y. Matsumura, H. Maeda, *Cancer Res.* **1986**, *46*, 6387.
[22] H. A. Santos, L. M. Bimbo, V. P. Lehto, A. J. Airaksinen, J. Salonen, J. Hirvonen, *Curr. Drug Discovery Technol.* **2011**, *8*, 228.
[23] H. C. Shum, D. Lee, I. Yoon, T. Kodger, D. A. Weitz, *Langmuir* **2008**, *24*, 7651.
[24] F. Kong, X. Zhang, M. Hai, *Langmuir* **2014**, *30*, 3905.
[25] W. G. Kaelin Jr., *Nat. Rev. Cancer* **2005**, *5*, 689.
[26] H. Pei, X. Zuo, D. Zhu, Q. Huang, C. Fan, *Acc. Chem. Res.* **2014**, *47*, 550.
[27] Q. Zhang, Q. Jiang, N. Li, L. Dai, Q. Liu, L. Song, J. Wang, Y. Li, J. Tian, B. Ding, Y. Du, *ACS Nano* **2014**, *8*, 6633.
[28] Q. Jiang, C. Song, J. Nangreave, X. Liu, L. Lin, D. Qiu, Z. G. Wang, G. Zou, X. Liang, H. Yan, B. Ding, *J. Am. Chem. Soc.* **2012**, *134*, 13396.
[29] W. J. Duncanson, T. Lin, A. R. Abate, S. Seiffert, R. K. Shah, D. A. Weitz, *Lab Chip* **2012**, *12*, 2135.
[30] D. Liu, S. Cito, Y. Zhang, C.-F. Wang, T. M. Sikanen, H. A. Santos, *Adv. Mater.* **2015**. doi: 10.1002/adma.201405408.
[31] L. M. Bimbo, E. Mäkilä, T. Laaksonen, V.-P. Lehto, J. Salonen, J. Hirvonen, H. A. Santos, *Biomaterials* **2011**, *32*, 2625.
[32] E. Winfree, F. Liu, L. A. Wenzler, N. C. Seeman, *Nature* **1998**, *394*, 539.
[33] D. Liu, E. Mäkilä, H. Zhang, B. Herranz, M. Kaasalainen, P. Kinnari, J. Salonen, J. Hirvonen, H. A. Santos, *Adv. Funct. Mater.* **2013**, *23*, 1893.
[34] A. Agarwal, M. A. Mackey, M. A. El-Sayed, R. V. Bellamkonda, *ACS Nano* **2011**, *5*, 4919.
[35] J. C. Kah, J. Chen, A. Zubieta, K. Hamad-Schifferli, *ACS Nano* **2012**, *6*, 6730.
[36] E. T. Castellana, R. C. Gamez, D. H. Russell, *J. Am. Chem. Soc.* **2011**, *133*, 4182.
[37] X. Huang, S. Neretina, M. A. El-Sayed, *Adv. Mater.* **2009**, *21*, 4880.
[38] H. Alhmoud, B. Delalat, R. Elnathan, A. Cifuentes-Rius, A. Chaix, M.-L. Rogers, J.-O. Durand, N. H. Voelcker, *Adv. Funct. Mater.* **2015**, *25*, 1137.
[39] B. Godin, C. Chiappini, S. Srinivasan, J. F. Alexander, K. Yokoi, M. Ferrari, P. Decuzzi, X. Liu, *Adv. Funct. Mater.* **2012**, *22*, 4186.

[40] B. Godin, E. Tasciotti, X. Liu, R. E. Serda, M. Ferrari, *Acc. Chem. Res.* **2011**, *44*, 979.
[41] R. E. Serda, B. Godin, E. Blanco, C. Chiappini, M. Ferrari, *Biochim. Biophys. Acta* **2011**, *1810*, 317.
[42] T. Tanaka, L. S. Mangala, P. E. Vivas-Mejia, R. Nieves-Alicea, A. P. Mann, E. Mora, H. D. Han, M. M. Shahzad, X. Liu, R. Bhavane, J. Gu, J. R. Fakhoury, C. Chiappini, C. Lu, K. Matsuo, B. Godin, R. L. Stone, A. M. Nick, G. Lopez-Berestein, A. K. Sood, M. Ferrari, *Cancer Res.* **2010**, *70*, 3687.
[43] E. Tasciotti, X. W. Liu, R. Bhavane, K. Plant, A. D. Leonard, B. K. Price, M. M. C. Cheng, P. Decuzzi, J. M. Tour, F. Robertson, M. Ferrari, *Nat. Nanotechnol.* **2008**, *3*, 151.
[44] R. Xu, Y. Huang, J. Mai, G. Zhang, X. Guo, X. Xia, E. J. Koay, G. Qin, D. R. Erm, Q. Li, X. Liu, M. Ferrari, H. Shen, *Small* **2013**.
[45] T. Zhou, M. Yu, B. Zhang, L. Wang, X. Wu, H. Zhou, Y. Du, J. Hao, Y. Tu, C. Chen, T. Wei, *Adv. Funct. Mater.* **2014**, *24*, 6922.
[46] B. Yang, S.-Y. Geng, X.-M. Liu, J.-T. Wang, Y.-K. Chen, Y.-L. Wang, J.-Y. Wang, *Soft Matter* **2012**, *8*, 518.
[47] H. L. Wong, N. Chattopadhyay, X. Y. Wu, R. Bendayan, *Adv. Drug Delivery Rev.* **2010**, *62*, 503.
[48] W. R. Greco, G. Bravo, J. C. Parsons, *Pharmacol. Rev.* **1995**, *47*, 331.